Proceedings of the International Conference on Oxide Materials for Electronic Engineering, May 29–June 2, 2017, Lviv

The Quasiparticle Electronic Energy Bands of the Cubic $KMgF_3$ Perovskite under Pressure Effect

S.V. Syrotyuk*, V.M. Shved and Yu.V. Klysko
Department of Semiconductor Electronics, Lviv Polytechnic National University, 79013 Lviv, Ukraine

First-principles calculations have been carried out to study the electronic properties of the $KMgF_3$ perovskite crystal. On first stage the calculations were performed within the generalized gradient approximation. On the second stage we have evaluated the quasiparticle corrections to the generalized gradient approximation band structure. These significantly improved electronic energies have been found here for the first time on base of the quasiparticle approach as implemented in the ABINIT code. Also, the pressure dependent parameters of electronic energy band spectra were found in the generalized gradient approximation. For the first time the pressure dependent electronic band energies have been evaluated within the quasiparticle approach. The generalized gradient approximation band gap parameters are in good agreement with the literature data, obtained with local density approximation or generalized gradient approximation exchange-correlation functionals and are much underestimated compared with the experiment. The quasiparticle band gap agrees well with the measured value.

DOI: 10.12693/APhysPolA.133.990
PACS/topics: 71.15.Ap, 71.15.Mb, 71.15.Qe

1. Introduction

$KMgF_3$ is an important material with a wide variety of technological applications, such as scintillator [1–4], dosimeter [5, 6], and window materials in the ultraviolet (UV) and vacuum-ultraviolet (VUV) wavelength region [7–9]. A theoretical study of the structural, electronic and optical properties of $KMgF_3$ was performed in [10] within the full-potential linearized augmented plane wave method (FP-LAPW). Electronic structures and absorption spectra for a perfect $KMgF_3$ crystal and a $KMgF_3$ crystal containing a potassium vacancy V_{-K} were calculated in [11] using CASTEP density functional theory code. First principles investigations of structural, electronic, elastic, and dielectric properties within the generalized gradient approximation (GGA) Perdew–Burke–Ernzerhof approach, with projector augmented wave (PAW) method, are presented in [12]. The electronic structures and absorption spectra on the polarized light in the perfect $KMgF_3$ crystal and the $KMgF_3$ crystal containing $V_(+ F)$ have been calculated using density functional theory code CASTEP with the lattice structure optimized [13]. High-pressure structural, elastic and electronic properties of the scintillator host material $KMgF_3$ were obtained in [14]. Investigation of the Fe^{3+} centers in perovskite $KMgF_3$ through a combination of *ab initio* (density functional theory) and semi-empirical (superposition model) calculations have been presented in work [15].

The objective of the present work, at the first stage, is to investigate the electronic structure of the perovskite $KMgF_3$ using the first-principles PAW approach within the GGA. At the second stage the aim of the work is to evaluate the improved electronic band energies by means of the Green function method, within the quasiparticle approximation (GW). The pressure effect on the electronic band energies, found within the GGA and GW, is also the problem to be solved in this research. The remainder of the paper is organized as follows: Sect. 2 describes the calculation method, Sect. 3 presents the results and a discussion of the electronic and finally, Sect. 4 summarizes the conclusions of this work.

*corresponding author; e-mail: svsnpe@yahoo.com

2. Computational details

2.1. The projector augmented waves

The PAW [16, 17] approach combines features of pseudopotential and the full-potential linearized augmented plane waves (FPLAPW) methods. The pseudo $|\tilde{\psi}_n(\boldsymbol{r})\rangle$ and all-electron $|\psi_n(\boldsymbol{r})\rangle$ functions are connected among themselves as follows:

$$|\psi_n(\boldsymbol{r})\rangle = |\tilde{\psi}_n(\boldsymbol{r})\rangle + \sum_a \sum_i \left(|\phi_i^a(\boldsymbol{r})\rangle - |\tilde{\phi}_i^a(\boldsymbol{r})\rangle\right) \langle \tilde{p}_i^a|\tilde{\psi}_n\rangle\,, \tag{1}$$

where $|\phi_i^a(\boldsymbol{r})\rangle$ is atomic wave function, $|\tilde{\phi}_i^a(\boldsymbol{r})\rangle$ is pseudowave function, and $\langle\tilde{p}_i^a|$ is a projector function. Summation in Eq. (1) is carried out over augmentation spheres, which are numbered with index a, and the index $i = \{n, l, m\}$ corresponds to the quantum numbers. As can be seen from Eq. (1):

$$|\psi_n(\boldsymbol{r})\rangle = \tau\,|\tilde{\psi}_n(\boldsymbol{r})\rangle\,, \tag{2}$$

where operator τ is given by the following equation [16, 17]:

$$\tau = 1 + \sum\sum \left(|\phi_i^a\rangle - |\tilde{\phi}_i^a\rangle\right) \langle \tilde{p}_i^a|\,. \tag{3}$$

Substituting the all-electron function defined by Eq. (2) into the Schrödinger equation

$$H\,|\psi_{n\boldsymbol{k}}\rangle = |\psi_{n\boldsymbol{k}}\rangle\,\varepsilon_{n\boldsymbol{k}}, \tag{4}$$

we obtain the transformed equation

$$\tau^{+}H\tau\,|\tilde{\psi}_{n\boldsymbol{k}}\rangle = \tau^{+}\tau\,|\tilde{\psi}_{n\boldsymbol{k}}\rangle\,\varepsilon_{n\boldsymbol{k}}, \tag{5}$$

which contains exactly the same electronic energy band spectrum $\varepsilon_{n\boldsymbol{k}}$ as in Eq. (4). Here n denotes the band number and $\boldsymbol{k}$ is a vector from the first Brillouin zone.

2.2. The quasiparticle energies

First, the electron energy $\varepsilon_{n\boldsymbol{k}}$ and eigenfunction $\psi_{n\boldsymbol{k}}$ are searched in the GGA approach from Eq. (6) [18, 19]:

$$(-\nabla^2 + V_{ext}(\boldsymbol{r}) + V_H(\boldsymbol{r}) + V_{xc}(\boldsymbol{r}))\varphi_{n\boldsymbol{k}}(\boldsymbol{r}) = \varepsilon_{n\boldsymbol{k}}\varphi_{n\boldsymbol{k}}(\boldsymbol{r}), \tag{6}$$

where $-\nabla^2$ is the kinetic energy operator, V_{ext} denotes the ionic pseudopotential, V_H and V_{xc} are the Hartree and exchange-correlation potential, respectively. Here n and $\mathbf{k}$ denote a band index and a wave vector in the Brillouin zone, respectively. The quasiparticle energies $E_{n\boldsymbol{k}}$ and eigenfunctions $\psi_{n\boldsymbol{k}}$ can be obtained from the quasiparticle Eq. (7) [18, 19]:

$$(-\nabla^2 + V_{ext}(\boldsymbol{r}) + V_H(\boldsymbol{r}))\,\psi_{n\boldsymbol{k}}(\boldsymbol{r}) + \int \Sigma(\boldsymbol{r},\boldsymbol{r'},E_{n\boldsymbol{k}})\,\psi_{n\boldsymbol{k}}(\boldsymbol{r'})d\boldsymbol{r'} = E_{n\boldsymbol{k}}\psi_{n\boldsymbol{k}}(\boldsymbol{r}), \tag{7}$$

where Σ is the non-local self-energy operator. The wave functions can be expanded as follows:

$$\psi_{n\boldsymbol{k}}(\boldsymbol{r}) = \sum_{n'} a_{nn'}\varphi_{n'\boldsymbol{k}}(\boldsymbol{r}). \tag{8}$$

From Eqs. (6)–(8) the perturbative quasiparticle Hamiltonian is obtained in the form

$$H_{nn'}(E) = \varepsilon_{n\boldsymbol{k}}\delta_{nn'} + \langle\varphi_{n\boldsymbol{k}}|\,\Sigma(E) - V_{xc}\,|\varphi_{n'\boldsymbol{k}}\rangle\,, \tag{9}$$

where the second term in Eq. (9) represents a perturbation.

The PAW functions have been generated for the following valence basis states: $\{3s^2 3p^6 4s^1 4p^0\}$for K, $\{2s^2 2p^6 3s^2 3p^0\}$for Mg, and $\{2s^2 2p^5\}$for F. All the PAW basis functions were obtained using the program *atompaw* [20]. The radii of the augmentation spheres r_{PAW} are 2.5, 1.4, and 1.4 a.u. for K, Mg, and F, respectively. The value of the lattice constant of the crystal $KMgF_3$ used in calculations equals 4.057 Å. We have derived it from minimization of the total energy $E(a)$ where a is a lattice parameter. Its value is well compared with the experimental one 3.987 Å [21]. For the other crystals, this parameter was obtained by minimization of the static lattice energy. The electronic energy bands have been evaluated by means of the ABINIT code [22, 23]. Integration over the Brillouin zone was performed on the Monkhorst-Pack [24] grid of 8 ×8 ×8 in the GWA and LDA calculation, respectively. The symmetry of the considered crystals $KMgF_3$ is described by space group $Pm\text{-}3m$ (number 221) and the Bravais lattice is cP (primitive cubic).

3. Results and discussions

Let us compare the results shown in Figs. 1, 2. The width of the upper part of the valence band obtained within the GGA (Fig. 1) equals approximately 3.5 eV. The corresponding GW value (Fig. 2) is 4.0 eV. The shortest distance between the upper part of the valence band and the nearest narrow core band (GGA, Fig. 1) is 5.5 eV. The corresponding GW value (Fig. 2) is 4.5 eV.

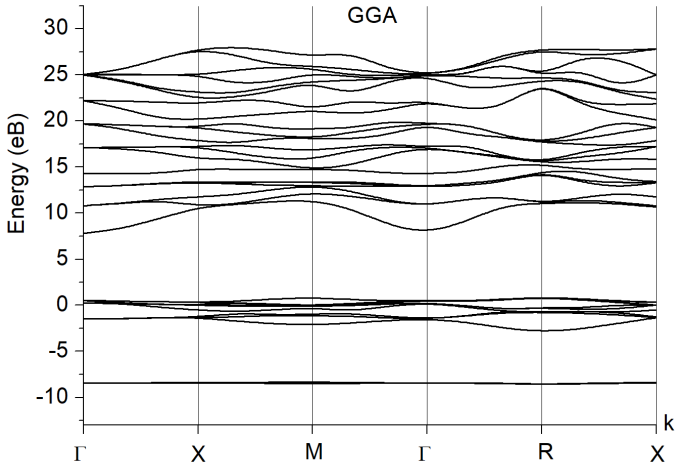

Fig. 1. Energy band structure of $KMgF_3$ obtained in the GGA approach at ambient pressure.

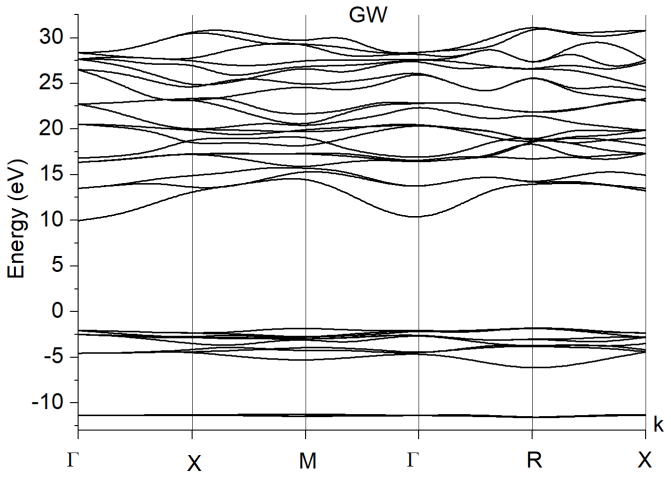

Fig. 2. Energy band structure of $KMgF_3$ obtained in the GW approach at ambient pressure.

Table I shows the electronic band gaps evaluated here (in first and fifth rows) and the values obtained in other research. As can be seen from Table I our GGA results are well compared with those obtained within GGA and LDA in other works. Deserve the attention differences in band gap values δE found here in the GW and GGA approaches. They are different for all the direct interband transitions.

TABLE I

Energies of interband transitions in the LDA and GW band structures of cubic perovskite $KMgF_3$ (in eV) obtained at ambient pressure. δE denotes the difference between the band gaps $E_g^{GW} - E_g^{GGA}$ obtained here.

	Γ–R	Γ–Γ	X–X	M–M	R–R
GGA	6.99	7.31	10.32	10.60	10.22
LDA [8]	7.27				
GGA [14]	6.95				
GGA [25]		7.68	10.68	11.00	10.38
GW	11.72	12.04	15.58	16.54	15.71
δE	4.73	4.73	5.26	5.94	5.49
Expt. [8]	10.8				

Our GW predicted fundamental indirect band gap is larger than the experimental one of 0.92 eV. One should be noted that long-wave value of the real part of dielectric function $\varepsilon_1(0) = 1.90$. Therefore, the crystal under consideration is an example of the weakly correlated electrons. Therefore, we can assume that the exciton binding energy is 0.92 eV.

At last, let us consider the pressure dependences for band gaps depicted in Figs. 3, 4. As can be seen from Fig. 3 the GGA approach assumes that the values of the interband gaps M-M and X-X at a pressure of 30 GPa should be approximately the same. However, this conclusion is not supported by a more precise theory of GW (Fig. 4). The band gaps X-X and R-R at an ambient pressure obtained within the GGA would be approximately equal (Fig. 3). However, the X-X gap is slightly less than R-R one, in the theory of GW, and they are approximately equal at a pressure 5 GPa (Fig. 4). We derived the interpolation formulae which express the value ε_g of the band gap,

$$\varepsilon_g = \mathrm{c_0 + c_1 p + c_2 p^2} \qquad (10)$$

for the GGA and GW pressure dependences. The respective coefficients are given in Table II. As can be seen from Figs. 3, 4 the curves corresponding transitions Γ–Γ and Γ–R are almost parallel. Mathematically, this fact is confirmed by almost equal coefficients c_1 (Table II) of linear summand in the formula (10).

TABLE II

The coefficients of the band gap approximation as a function of pressure calculated by the formula (10).

	GGA			GW		
	c_0	c_1	c_2	c_0	c_1	c_2
Γ–R	6.99	0.053	0.00043	11.72	0.061	0.00043
Γ–Γ	7.31	0.054	0.00039	12.04	0.061	0.00038
X–X	10.32	0.052	0.00012	15.58	0.064	0.00013
M–M	10.60	0.046	0.000030	16.54	0.056	0.000099
R–R	10.22	0.030	0.000042	15.71	0.039	0.000012

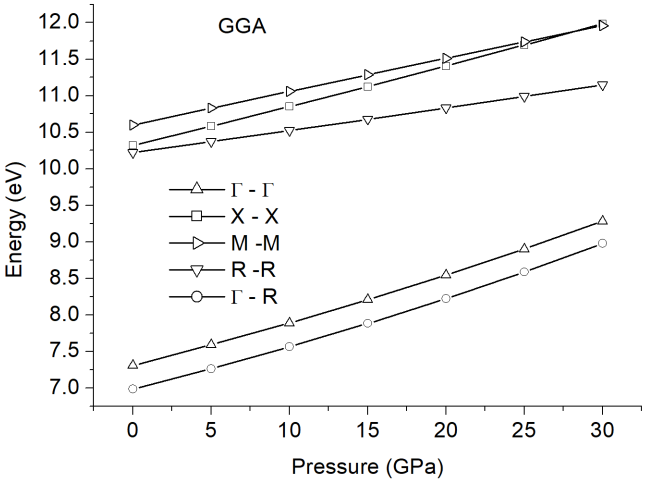

Fig. 3. Pressure dependence of band gaps in $KMgF_3$ evaluated within the GGA formalism.

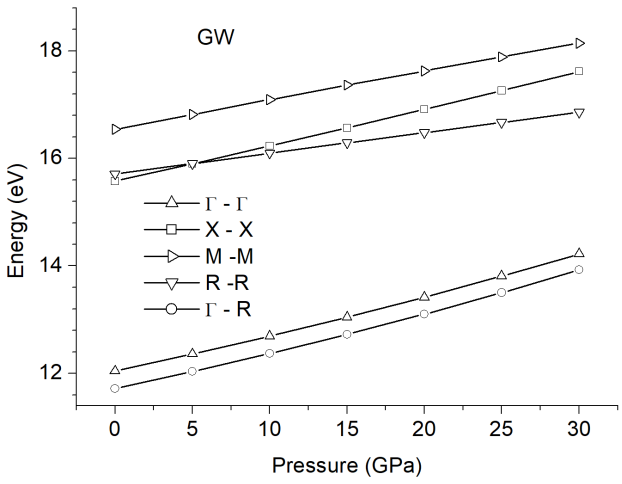

Fig. 4. Pressure dependence of band gaps in $KMgF_3$ evaluated within the quasiparticle GW theory.

4. Summary and conclusions

For the first time for the crystal $KMgF_3$ the quasiparticle electronic energy bands have been evaluated. The values of interband gaps were found depending on the hydrostatic pressure. The band gaps found here in the GGA are well compared with results obtained in other works. All the LDA and GGA band gap values are much underestimated with respect to available experimental data. In particular, for the crystal $KMgF_3$, we obtained the value of the indirect band gap of 6.99 eV within the framework of the GGA approach. Than we have calculated the improved electronic energy bands by means of the GW approach. The corresponding value of the band gap is 11.72 eV and is in much closer agreement with the experimental one (10.8 eV) than the obtained here GGA result. The band gap value evaluated within the GW approach exceeds the experiment by 0.92 eV. Therefore, we

can estimate the exciton binding energy, which is equal to 0.92 eV. The interpolation formulae for pressure dependences of lowest interband transition energies have been derived for all the direct and indirect band gaps. The differences δE (Table I) significantly depend on the wave vector, so the use of the scissor operator may be characterized by some uncertainty.

References

[1] A.V. Gektin, *J. Lumin.* **87**, 1283 (2000).

[2] M. Yamaga, M. Honda, N. Kawamata, T. Fujita, K. Shimamura, T. Fukuda, *J. Phys. Condens. Matter* **13**, 3461 (2001).

[3] S. Mahlik, K. Wisniewski, M. Grinberg, Hyo Jin Seo, *Opt. Mater.* **33**, 996 (2011).

[4] D.J. Daniel, U. Madhusoodanan, O. Annalakshmi, M.T. Jose, P. Ramasamy, *Opt. Mater.* **45**, 224 (2015).

[5] N.J.M. Le Masson, A.J.J. Bos, C.W.E. Van Eijk, C. Furetta, J.P. Chaminade, *Radiat. Protect. Dosim.* **100**, 229 (2002).

[6] M. Martini, F. Meinardi, A. Scacco, *Chem. Phys. Lett.* **293**, 43 (1998).

[7] M.D. Whitfeld, S.P. Lansley, O. Gaudin, R.D. McKeag, N. Rizvi, R.B. Jackman, *Diam. Relat. Mater.* **10**, 693 (2001).

[8] T. Nishimatsu, N. Terakubo, H. Mizuseki, Y. Kawazoe, D.A. Pawlak, K. Shimamura, T. Fukuda, *Jpn. J. Appl. Phys.* **41**, 365 (2002).

[9] H. Sato, A. Bensalah, N. Solovieva, A. Beitlerova, A. Vedda, M. Martini, M. Nikl, T. Fukuda, *Radiat. Meas.* **38**, 463 (2004).

[10] M. Sahnoun, M. Zbiri, C. Daul, R. Khenata, H. Baltache, M. Driz, *Mater. Chem. Phys.* **91**, 185 (2005).

[11] F. Cheng, T.-Y. Liu, Q.-R. Zhang, H.-L. Qiao, X.-W. Zhou, *Chin. Phys. Lett.* **28**, 3 (2011).

[12] G. Pilania, V. Sharma, *J. Mater. Sci.* **48**, 7635 (2013).

[13] F. Cheng, T. Liu, Q. Zhang, H. Qiao, X. Zhou, *Nucl. Instrum. Methods Phys. Res. B* **268**, 2403 (2010).

[14] G. Vaitheeswaran, V. Kanchana, R.S. Kumar, A.L. Cornelius, M.F. Nicol, A. Svane, A. Delin, B. Johansson, *Phys. Rev. B* **76**, 014107 (2007).

[15] Y. Emül, D. Erbahar, M. Açıkgöz, *J. Appl. Phys.* **118**, 063903 (2015).

[16] P.E. Blöchl, *Phys. Rev. B* **50**, 17953 (1994).

[17] M. Torrent, F. Jollet, F. Bottin, G. Zerah, X. Gonze, *Comput. Mater. Sci.* **42**, 337 (2008).

[18] B. Arnaud, M. Alouani, *Phys. Rev. B* **62**, 4464 (2000).

[19] M. Shishkin, G. Kresse, *Phys. Rev. B* **74**, 035101 (2006).

[20] A.R. Tackett, N.A.W. Holzwarth, G.E. Matthews, *Comput. Phys. Commun.* **135**, 348 (2001).

[21] K.S. Aleksandrov, A.T. Anistratov, B.V. Beznosikov, N.V. Fedoseeva, *Phase Transitions in the Crystals of Halide Compounds ABX_3*, Science, Novosibirsk 1981 (in Russian).

[22] X. Gonze, B. Amadon, P.-M. Anglade, J.-M. Beuken, F. Bottin, P. Boulanger, F. Bruneval, D. Caliste, R. Caracas, M. Cote, T. Deutsch, L. Genovese, Ph. Ghosez, M. Giantomassi, S. Goedecker, D.R. Hamann, P. Hermet, F. Jollet, G. Jomard, S. Leroux, M. Mancini, S. Mazevet, M.J.T. Oliveira, G. Onida, Y. Pouillon, T. Rangel, G.-M. Rignanese, D. Sangalli, R. Shaltaf, M. Torrent, M.J. Verstraete, G. Zerah, J.W. Zwanziger, *Comput. Phys. Commun.* **180**, 258 (2009).

[23] X. Gonze, F. Jollet, F. Abreu Araujo, D. Adams, B. Amadon, T. Applencourt, C. Audouze, J.-M. Beuken, J. Bieder, A. Bokhanchuk, E. Bousquet, F. Bruneval, D. Caliste, M. Cote, F. Dahm, F. Da Pieve, M. Delaveau, M. Di Gennaro, B. Dorado, C. Espejo, G. Geneste, L. Genovese, A. Gerossier, M. Giantomassi, Y. Gillet, D.R. Hamann, L. He, G. Jomard, J. Laflamme Janssen, S. Le Roux, A. Levitt, A. Lherbier, F. Liu, I. Lukacevic, A. Martin, C. Martins, M.J.T. Oliveira, S. Poncè, Y. Pouillon, T. Rangel, G.-M. Rignanese, A.H. Romero, B. Rousseau, O. Rubel, A.A. Shukri, M. Stankovski, M. Torrent, M.J. Van Setten, B. Van Troeye, M.J. Verstraete, D. Waroquiers, J. Wiktor, B. Xu, A. Zhou, J.W. Zwanziger, *Computer Phys. Comm.* **205**, 106 (2016).

[24] H.J. Monkhorst, J.D. Pack, *Phys. Rev. B* **13**, 5188 (1976).